
1-15-2020

Tracing Dehydration and Melting of the Subducted Slab with Tungsten Isotopes in Arc Lavas

Sarah E. Mazza
Smith College, smazza@smith.edu

Andreas Stracke
Westfälische Wilhelms-Universität Münster

James B. Gill
University of California, Santa Cruz

Jun Ichi Kimura
Japan Agency for Marine-Earth Science and Technology

Thorsten Kleine
Westfälische Wilhelms-Universität Münster

Follow this and additional works at: https://scholarworks.smith.edu/geo_facpubs



Part of the [Geology Commons](#)

Recommended Citation

Mazza, Sarah E.; Stracke, Andreas; Gill, James B.; Kimura, Jun Ichi; and Kleine, Thorsten, "Tracing Dehydration and Melting of the Subducted Slab with Tungsten Isotopes in Arc Lavas" (2020). Geosciences: Faculty Publications, Smith College, Northampton, MA. https://scholarworks.smith.edu/geo_facpubs/111

This Article has been accepted for inclusion in Geosciences: Faculty Publications by an authorized administrator of Smith ScholarWorks. For more information, please contact scholarworks@smith.edu



Tracing dehydration and melting of the subducted slab with tungsten isotopes in arc lavas



Sarah E. Mazza^{a,b,*}, Andreas Stracke^c, James B. Gill^d, Jun-Ichi Kimura^e, Thorsten Kleine^a

^a Institut für Planetologie, University of Münster, 48149 Münster, Germany

^b Department of Geosciences, Smith College, Northampton, MA 01063, USA

^c Institut für Mineralogie, University of Münster, 48149 Münster, Germany

^d Department of Earth and Planetary Sciences, University of California Santa Cruz, Santa Cruz, CA 95064, USA

^e Japan Agency for Marine-Earth Science and Technology, Yokosuka 237-0061, Japan

ARTICLE INFO

Article history:

Received 26 April 2019

Received in revised form 3 October 2019

Accepted 30 October 2019

Available online 15 November 2019

Editor: R. Dasgupta

Keywords:

stable tungsten isotopes

arc volcanism

slab dehydration

volatile recycling

ABSTRACT

Tungsten is strongly incompatible during magmatic processes and is fluid mobile in subduction zones. Here we show that W isotope fractionation in arc lavas provide a powerful new tool for tracing slab dehydration and melting in subduction zones. Geochemically well characterized, representative arc-lavas from three subduction zones were chosen for this study to evaluate W isotope fractionation under different sub-arc conditions. Arc-lavas from SW Japan are produced by subducting a young, hot slab, and lavas from the volcanic front and rear arc of the Sangihe and Izu arcs are produced during subduction of a cold slab. The heaviest W isotope compositions ($\delta^{184}\text{W} \sim 0.06\%$) are observed in fluid-rich samples from the volcanic fronts of the Sangihe and Izu arcs. With increasing distance from the volcanic front, more melt-rich samples are characterized by progressively lighter W isotope compositions. Enriched alkali basalts from SW Japan, thought to be the product of mantle melting at a slab tear, and adjacent shoshonites have the lightest W isotope compositions ($\delta^{184}\text{W} \sim 0\%$). The correlation of W isotope fractionation with various indices of fluid release (e.g., Ce/Pb, Ba/Th) suggests that the heavy W isotope signatures record fluid recycling near the volcanic front due to dehydration of the subducted slab. Upon release of the heavy W, the residual slab preferentially retains isotopically light W, which is released during subsequent melting of drier lithologies in hot subduction zones, such as SW Japan. These data suggest that W isotopes can be used as a tracer of slab dehydration, potentially helping to determine the onset of cold subduction zone magmatism and hence, modern-style plate tectonics.

© 2019 The Authors. Published by Elsevier B.V. This is an open access article under the CC BY-NC-ND license (<http://creativecommons.org/licenses/by-nc-nd/4.0/>).

1. Introduction

On modern Earth, new continental lithosphere forms at subduction zones. The subducting sediments or altered oceanic crust (AOC) release aqueous fluids and hydrous silicate melts, which are transported into the mantle wedge, where hydrous melting produces arc volcanics (Gill, 1981; Tatsumi and Eggins, 1995; Grove et al., 2012). Depending on the local subducted components and the pressure-temperature (P-T) conditions during subduction (Syracuse et al., 2010), arc magmas have different geochemical signatures. The residual subducted slab transports elements back into the mantle, and thus plate subduction is also the main mechanism for crust-mantle exchange since the onset of plate tectonics.

The P-T conditions during subduction play an important role for geochemical cycling between crust and mantle, especially for water. Numerical models have shown that dehydration is incomplete beneath the volcanic front of cold subduction zones, allowing the hydrated lower crust and underlying mantle to recycle water deep into the mantle (van Keken et al., 2011). In contrast, hot subduction zones undergo shallower dehydration and more extensive melting of the slab; aqueous fluids are released by dehydration of subducted serpentinites and facilitate flux melting within the slab and overlying mantle wedge (Spandler and Pirard, 2013). The trace element signatures of arc magmas record these dehydration reactions, and thus reflect the pressure-temperature conditions during fluid release from the subducting slab (e.g., Plank et al., 2009). However, the mechanism and location of fluid release from the subducting slab remains poorly understood. Hence, novel techniques may help to further constrain slab dehydration mechanisms.

The mass-dependent isotope fractionation of fluid-mobile elements such as Mo may improve our understanding of dehydration

* Corresponding author at: Department of Geosciences, Smith College, Northampton, MA 01063, USA.

E-mail address: smazza@smith.edu (S.E. Mazza).

melting in arcs because the slab-fluid component in some volcanic fronts is characterized by heavy Mo isotope compositions (e.g., Willbold and Elliott, 2017). However, crystal fractionation of amphibole during arc magma evolution may also produce heavy Mo isotope ratios (Wille et al., 2018), and so Mo isotope ratios in arc lavas may not be a unique proxy for slab dehydration. Tungsten has similar properties as Mo, but is less affected by magmatic differentiation, and thus W stable isotope ratios may be less ambiguous for tracing slab dehydration.

Tungsten is highly incompatible during magmatic processes (Newson et al., 1996; Arevalo and McDonough, 2008), thus enriched in the continental crust (~1 ppm, Rudnick and Gao, 2003) relative to the mantle (~12 ppb, König et al., 2011). Experiments have shown that W strongly partitions into aqueous fluids, independent of fO_2 and salinity (Bali et al., 2012). This is consistent with the observation that magmas produced in subduction zones are enriched in W relative to the depleted mantle (König et al., 2008, 2011). In some cases, W enrichment in arc lavas is proportional to the amount of fluid in the system, in others it is probably due to melting of subducted sediments (König et al., 2008). If W mobilization by dehydration causes stable isotope fractionation, or if the W mobilized from different parts of the subducted slab is isotopically variable, W isotope ratios could be a powerful new tool for investigating material transport from the slab into the mantle wedge, and ultimately arc volcanics.

In this study we investigate the W stable isotope composition in arc magmas to better constrain the nature and extent of W isotope fractionation in subduction zones. Using well-characterized arc lavas that allow for distinguishing between fluid and sediment dominated arc magma sources, we explore a variety of mechanism that could be responsible for W isotope fractionations and use our data for distinguishing isotope fractionations due to temperature-dependent dehydration of the slab from inherited signatures resulting from seawater alteration and subducted sediments.

2. Geological background and sample selection

Well-characterized, representative volcanic rocks from three different subduction zones were chosen to trace W stable isotope fractionation in different subduction zones. The bulk rock compositions are reported in Supplementary Table 1. The Izu and Sangihe arcs are cold subduction zones, according to the classification of Syracuse et al. (2010) who determine the thermal characteristic of arcs with parameters such as convergence speed (4.6 cm/yr for the Izu arc and 4.0 cm/yr for the Sangihe arc), slab dip (45° for the Izu arc and 55° for the Sangihe arc), and age of the subducting lithosphere (>100 Ma for the Izu arc and >60 Ma for the Sangihe arc). The Izu arc samples are three basaltic andesites from the northernmost volcanic front (Oshima), including the Geological Survey of Japan (GSJ) standard JB-2, and three rear-arc basalts from 70–110 km behind the front (Fig. 1b). Three of the samples from the Sangihe arc are from the southern to central volcanic front stretching ~200 km along the arc. The other two are basalts from ~50 km behind the southern front (Fig. 1c). At both the Izu and Sangihe arcs, aqueous slab-derived fluids dominate the geochemical signatures of the volcanic front lavas, and slab-melt components dominate the rear arc lavas (Tollstrup et al., 2010; Freymuth et al., 2016; Morrice et al., 1983; Hanyu et al., 2012 and references within).

The Izu and Sangihe arcs are intra-oceanic arcs with no evidence of old continental crust. Hence, contamination by such crust does not affect magma evolution. Trace element abundances suggest that rutile is residual in the slab of both arcs (Tollstrup et al., 2010; Hanyu et al., 2012). The slab flux for the two arcs transitions from low temperature aqueous fluid to high temperature supercritical fluid/melt with increasing depth of the subducting plate, as indicated by enriched Ba/La, Ba/Th, Nb/Zr, $^{206}\text{Pb}/^{204}\text{Pb}$, signatures

for the volcanic front and enriched La/Yb, and Ce/Pb for the rear arc of both the Izu and Sangihe arcs (full discussion in Tollstrup et al., 2010; Hanyu et al., 2012; La/Yb versus Ba/La in Fig. 2). The source of the slab components differs slightly: the Sangihe source is estimated as 20% sediment and 80% AOC (Hanyu et al., 2012) whereas the Izu rear arc source is estimated as 5% sediment and 95% AOC (Tollstrup et al., 2010). Tectonically, the greatest differences between the two arcs are the lack of back arc spreading behind the Sangihe arc, and the presence of a much thicker sediment prism in front of it.

In contrast, SW Japan is an example of a 'hot' subduction zone due to the shallow slab angle (<30°) and youth (20 Ma) of the subducting Shikoku Basin (Syracuse et al., 2010). A large variety of lithologies occur in different areas of the SW Japan arc that differ from those found in 'cold' subduction zones (e.g., Izu and Sangihe). Samples used in this study were characterized by Kimura et al. (2014, 2015) and include two ocean island basalt-type (OIB) basalts and two shoshonites from Abu, one adakite from Aono, and two adakites from Daisen volcano (Fig. 1b), all of which are unaffected by crustal contamination. The adakites and similar Setouchi high-magnesium andesites (HMA, represented by the GSJ reference material JA-2) have the largest mass fraction of sediment in the slab source (from ~30% sediment in the adakites up to 95% sediment in the HMAs), and the highest water content in the slab melt (up to 3 wt% H₂O, Fig. 3a) (Kimura et al., 2014). The Abu shoshonites and OIB-type basalts have the least slab component of all analyzed SW Japan rocks (Fig. 3c; Kimura et al., 2014). They erupted above a region where the subducting slab is absent in seismic tomography images, suggesting that they were produced above a slab tear (Zhao et al., 2012; Kimura et al., 2014).

While the focus of this study is to characterize W stable isotope ratios in active subduction zones, we included 6 OIBs to evaluate W isotope fractionation due to the recycling and long-term storage of subducted lithologies in the mantle. We selected representative OIBs from the Cook-Austral and Tristan-Gough hotspot tracks. Both of these hotspots are the result of mantle plumes, thermal anomalies that originate at great depth in the mantle (e.g., French and Romanowicz, 2015). The OIB samples represent geochemical heterogeneities in the mantle, which have been grouped into different categories based on their major, trace element and radiogenic isotopes compositions (Pb-Sr-Nd) (e.g. Zindler and Hart, 1986; Willbold and Stracke, 2006; Jackson and Dasgupta, 2008, and references within). These categories are high μ ($\mu = ^{238}\text{U}/^{204}\text{Pb}$; HIMU) and different varieties of enriched mantle (EM). HIMU is thought to be the product of recycling oceanic lithosphere (e.g. Zindler and Hart, 1986), uniform in both major (Jackson and Dasgupta, 2008) and trace element composition (Willbold and Stracke, 2006). The EM reservoirs are thought to be the product of recycling continental crust into the mantle (cf. Stracke, 2012). We investigate two HIMU-type samples (from the islands of Mangaia and Rurutu of the Cook-Austral), two EM-like samples (from the islands of Atiu and Rarotonga of the Cook-Austral), and two EM1-type samples (from Tristan da Cunha and Gough islands) (Willbold and Stracke, 2006).

3. Methods

Fresh, unaltered rock fragments were processed in an agate shatterbox for samples from Sangihe, Izu, and SW Japan, as well as the OIBs. Geological Survey of Japan rock reference materials JB-2 and JA-2 were used as unknowns in this study, and were processed in high-alumina mills (Ando et al., 1987). The chemical composition of the OIBs were acquired following the procedure described in Willbold and Stracke (2006). For the W isotope analyses, rock powders (~0.07–0.5 g) were spiked with a ^{180}W - ^{183}W double spike prior to digestion. Samples were dissolved in 2:1 HF-

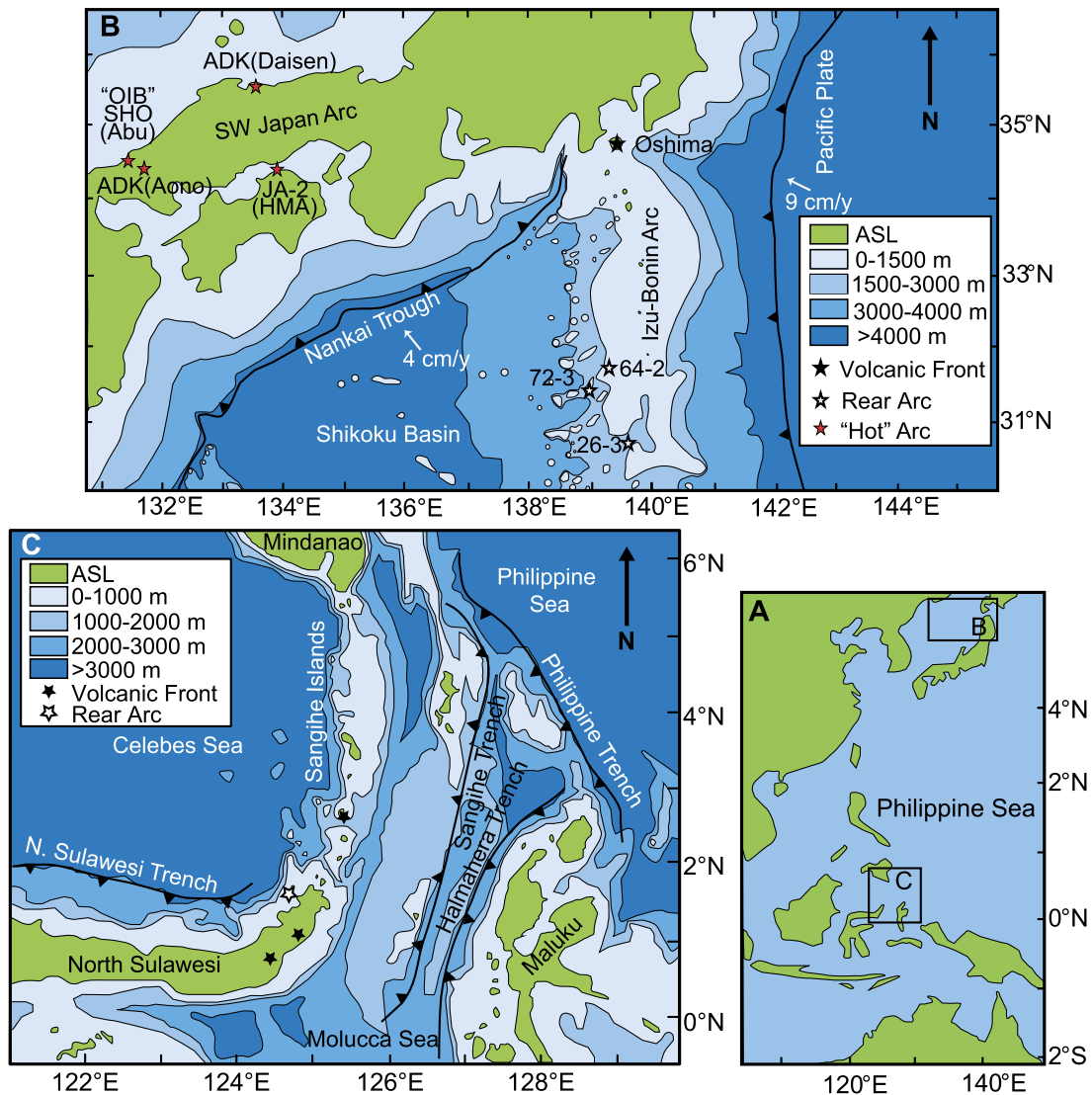


Fig. 1. Maps showing sample locations. **A)** Map of the Philippine Sea showing Japan and Indonesia. **B)** Bathymetric map of Japan and Izu-Bonin arc. SHO: shoshonite, "OIB": Abu OIB-like, ADK: Adakite, HMA: High Mg Andesite. **C)** Bathymetric map of the Sangihe arc. (For interpretation of the colors in the figure(s), the reader is referred to the web version of this article.)

HNO_3 at 150°C for at least 48 hours. Tungsten was separated from the sample matrix using a three-stage anion exchange chromatography following the protocols developed by Krabbe et al. (2017). Tungsten isotope measurements were performed with a Neptune Plus MC-ICPMS at the Institut für Planetologie in Münster, using an Aridus II sample introduction system. Each sample measurement was bracketed by measurements of an optimally spiked external standard solution (NIST 3163 W, provided by the National Institute of Standard and Technology). Data reduction was performed in MATLAB using the *Double Spike Toolbox* (Rudge et al., 2009) with an add-in script that iteratively corrects for Hf-interference (Krabbe et al., 2017). Data are reported as $\delta^{184}\text{W}$, which is the per mil deviation of $^{184}\text{W}/^{183}\text{W}$ from the NIST 3163 W standard (Table 1).

Different aliquots of the same sample powder were dissolved in duplicate or triplicate, and measured at least 4 times per dissolution, with the total analyses per sample ranging from 8-13 measurements. The reference material JB-2 was dissolved without prior leaching 5 times (~ 0.5 g of powder per digestion) with 28 total analyses run over a 12-month period. The W yield for these procedures was between 60-95%. Total procedural blanks ranged between 100-200 pg of W and were insignificant.

Repeated measurements of the spiked NIST 3163 standard solution yielded a reproducibility of ± 0.018 on $\delta^{184}\text{W}$ (2 S.D.) for 400 analyses from 8 different analytical sessions spanning the course of 14 months (Supplementary Fig. 1a). The accuracy and precision for samples of the W isotope measurements for samples were evaluated by the repeat analyses of JB-2, with an average $\delta^{184}\text{W}$ of 0.057 ± 0.025 (2 S.D.) (Supplementary Fig. 1b). Similar to Mo stable isotopes measurements (Willbold and Elliott, 2017), JB-2 therefore may serve as a reliable standard for W stable isotope measurements.

Few laboratories have measured W stable isotopes in terrestrial rocks (Irisawa and Hirata, 2006; Breton and Quitté, 2014; Abraham et al., 2015; Krabbe et al., 2017; Kurzweil et al., 2018; 2019). Of these, Abraham et al. (2015) and Kurzweil et al. (2018) developed a W double spike technique that is similar to the methods used for this study (Krabbe et al., 2017). Both Kurzweil et al. (2018) and Krabbe et al. (2017) reported values for USGS reference materials AGV-2 and BHVO-2 which are within analytical uncertainty of each other. Abraham et al. (2015) also measured AGV-2, but they observe two times larger fractionations than Krabbe et al. (2017) and Kurzweil et al. (2018). Although these previous studies did not report data for JB-2, the good agreement of data for AGV-2 show that

Table 1
Tungsten concentration (ppm) and W isotope composition.

Sample ID	Location	W (ppm)	$\delta^{184}\text{W}$	95% confidence	n = replicates (analyses)
JB-2	Izu Arc - Oshima	0.302	0.057	0.005	n = 5 (28)
1986A-1	Izu Arc - Oshima	0.213	0.056	0.005	n = 2 (9)
N4-1	Izu Arc - Oshima	0.199	0.060	0.008	n = 2 (8)
IRA 72-3	Izu Arc - Back Arc Knoll	0.816	0.021	0.006	n = 3 (12)
IRA 64-2	Izu Arc - Back Arc Knoll	0.191	0.058	0.006	n = 2 (10)
IRA 26-3	Izu Arc - Back Arc Knoll	0.084	0.077	0.014	n = 2 (10)
PJ-83-77	Sangehi Arc - Buhias Pahepa	0.131	0.072	0.005	n = 3 (12)
MM-80-27	Sangehi Arc - Sopotan	0.077	0.058	0.006	n = 3 (12)
PJ-186-77	Sangehi Arc - Ambang	0.487	0.059	0.006	n = 3 (13)
PJ-125-77	Sangehi Arc - Manado Tua	0.165	0.041	0.005	n = 3 (11)
TKK15A	Sangehi Arc - Manado Tua	0.418	0.054	0.009	n = 3 (13)
71 Daisen	SW Japan - Karasugasen	0.599	0.042	0.007	n = 2 (11)
89 Daisen	SW Japan - Karasugasen	0.421	0.054	0.014	n = 2 (12)
100 Aono	SW Japan - Aonoyama	0.239	0.033	0.003	n = 2 (9)
JA-2	SW Japan - SRM	1.022	0.034	0.013	n = 2 (10)
301 Abu	SW Japan - Katamata	0.377	0.009	0.006	n = 2 (10)
303 Abu	SW Japan - Katamata	0.394	0.017	0.012	n = 2 (10)
320 Abu	SW Japan - Sugi	0.427	0.001	0.010	n = 2 (12)
322 Abu	SW Japan - Tatamigafuchi	0.417	0.007	0.008	n = 2 (8)
RRT130	Rururtu	0.296	0.03	0.01	n = 2 (9)
MGA108	Mangaia	0.419	0.048	0.008	n = 2 (8)
T 122	Tristan da Cunha	0.63	0.046	0.006	n = 2 (7)
G 131	Gough	0.602	0.024	0.013	n = 2 (6)
ATU128	Atiu	0.356	0.048	0.008	n = 2 (9)
RTG161	Rarotonga	0.755	0.036	0.007	n = 3 (13)

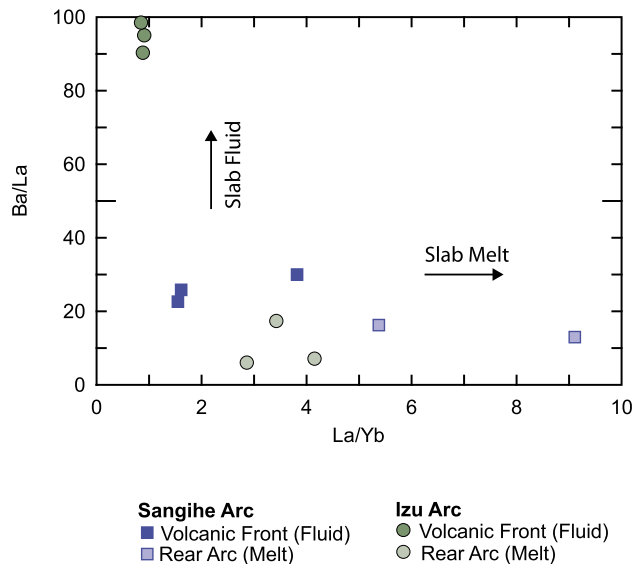


Fig. 2. Classic subduction zone discrimination plots for slab-flux showing increased slab-melt fluxing agent with increased La/Yb and increasing slab-fluid fluxing agent with increased Ba/La. Samples from the rear arc in both the Izu and Sangihe arcs are characterized by a slab-melt fluxing agent as indicated by increasing La/Yb with low Ba/La. The volcanic front in both arcs are characterized by a slab-fluid, with Oshima (Izu) having the strongest fluid signature of all the samples analyzed in this study.

the data of this study (which uses the same method as Krabbe et al., 2017) and Kurzweil et al. (2018) are consistent with each other.

4. Results

To evaluate the extent and direction of W stable isotope fractionation in natural samples, a suitable reference is required. As will be discussed in more detail below, the average chondritic $\delta^{184}\text{W}$ value of $0.031 \pm 0.007\text{‰}$ (Krabbe et al., 2017) is likely representative for the W stable isotope composition of bulk sili-

cate Earth (BSE), which is the most suitable reference composition for assessing mass-dependent W isotope variation in terrestrial igneous rocks. We refer to samples that have higher $\delta^{184}\text{W}$ values than BSE (and chondrites) as isotopically “heavy”, and samples with lower values as isotopically “light” (Fig. 4).

All but one of the Izu and Sangihe arc samples have heavy $\delta^{184}\text{W}$ values (Fig. 4). Both arcs are characterized by an aqueous-fluid rich volcanic front and a slab-melt rich rear arc, as inferred from the increasing Ce/Pb and decreasing Ba/La associated with increasing distance from the trench. Therefore, higher $\delta^{184}\text{W}$ values are associated with aqueous-fluid rich lavas, and lower $\delta^{184}\text{W}$ values are associated with slab-melt rich lavas in both arcs (Fig. 5, Fig. 6). Of the Izu and Sangihe arc samples, sample 72-3 has the lightest $\delta^{184}\text{W}$ signature; this sample is located the farthest behind the volcanic front and has the highest Ce/Pb.

In SW Japan, a ‘hot’ subduction zone, arc lavas have uniformly lower $\delta^{184}\text{W}$ values for a given Ce/Pb than the Izu and Sangihe arc lavas (Fig. 5). The Daisen adakites have the heaviest $\delta^{184}\text{W}$ values for SW Japan, comparable to the Izu and Sangihe rear arc samples (Fig. 4). These samples are also characterized by the highest slab liquid water content (Fig. 3, Fig. 5) and the most slab liquid added to the mantle wedge. The lightest $\delta^{184}\text{W}$ values are measured in the Abu OIB-type and shoshonites lavas, which have the lowest slab liquid water content and the least amount of slab liquid (Fig. 3, Fig. 5).

There is no correlation between SiO_2 content and $\delta^{184}\text{W}$ values (Supplementary Fig. 2), indicating that magmatic differentiation does not affect $\delta^{184}\text{W}$ in oceanic arcs, unlike previous suggestions (Krabbe et al., 2017; Kurzweil et al., 2018). There is also no correlation between $\delta^{184}\text{W}$ values and W/Th ratios (Fig. 7).

The OIB have a narrow, yet analytically resolvable range of $\delta^{184}\text{W}$ values, from $\delta^{184}\text{W} 0.024 \pm 0.013\text{‰}$ to $0.048 \pm 0.008\text{‰}$ (Fig. 4). Half of the OIBs measured fall within uncertainty of the chondritic value, while the other half are slightly heavier. There is no obvious correlation between $\delta^{184}\text{W}$ values and radiogenic isotope category, because both HIMU and EM-type OIB cover the full range of the observed $\delta^{184}\text{W}$ OIB values.

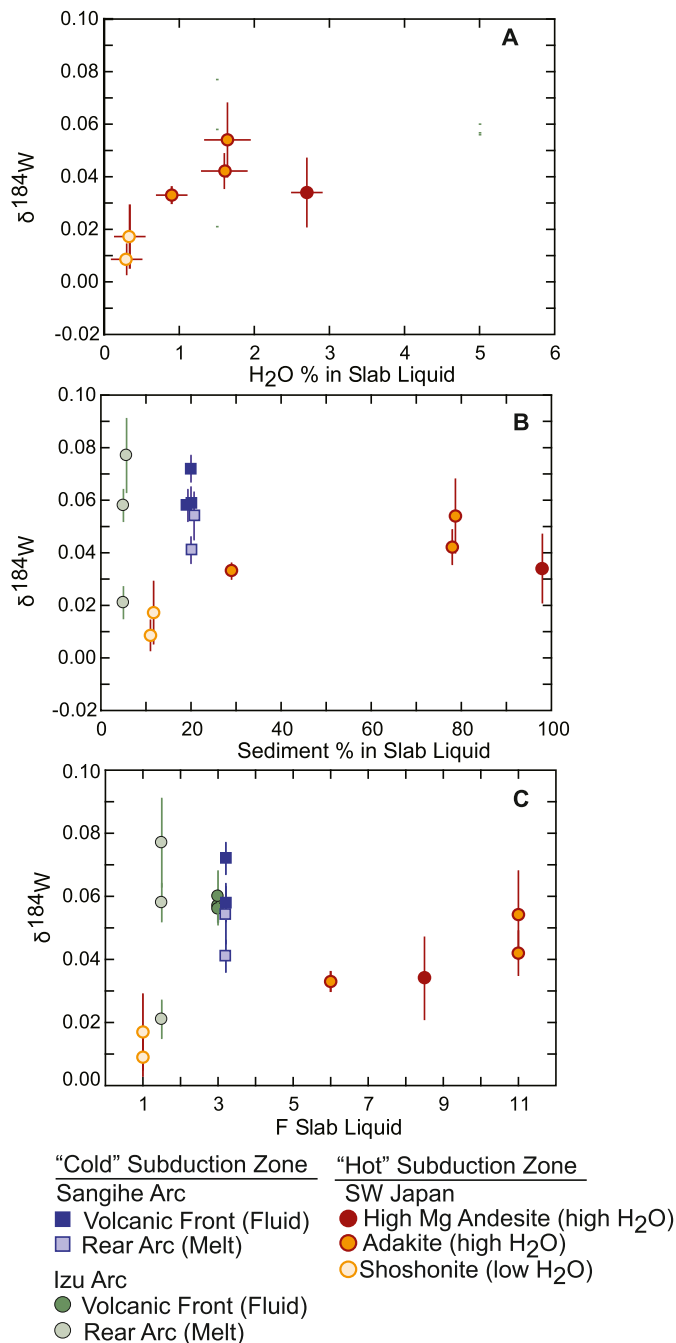


Fig. 3. **A)** Modeled amount of water in the slab liquid for SW Japan (Kimura et al., 2014) compared to the $\delta^{184}\text{W}$ composition. **B)** Modeled amount of sediment in the slab liquid for SW Japan (Kimura et al., 2014), Sangihe (Hanyu et al., 2012), and Izu (Tollstrup et al., 2010) compared to $\delta^{184}\text{W}$ composition. **C)** Modeled mass fraction (F) of slab liquid in the mantle source for SW Japan (Kimura et al., 2014), Sangihe (Hanyu et al., 2012), and Izu (Kimura et al., 2010) compared to $\delta^{184}\text{W}$ composition.

5. Discussion

5.1. The W stable isotope composition of Earth's mantle and bulk silicate Earth

The W stable isotope composition of the BSE should be similar to that of chondritic meteorites if sequestering W into the core by high-T metal-silicate separation did not induce W isotope fractionation. As observed for Mo, stable isotope fractionation at the high-T conditions during metal-silicate separation and core formation in Earth is negligible (Burkhardt et al., 2014; Hin et al., 2013;

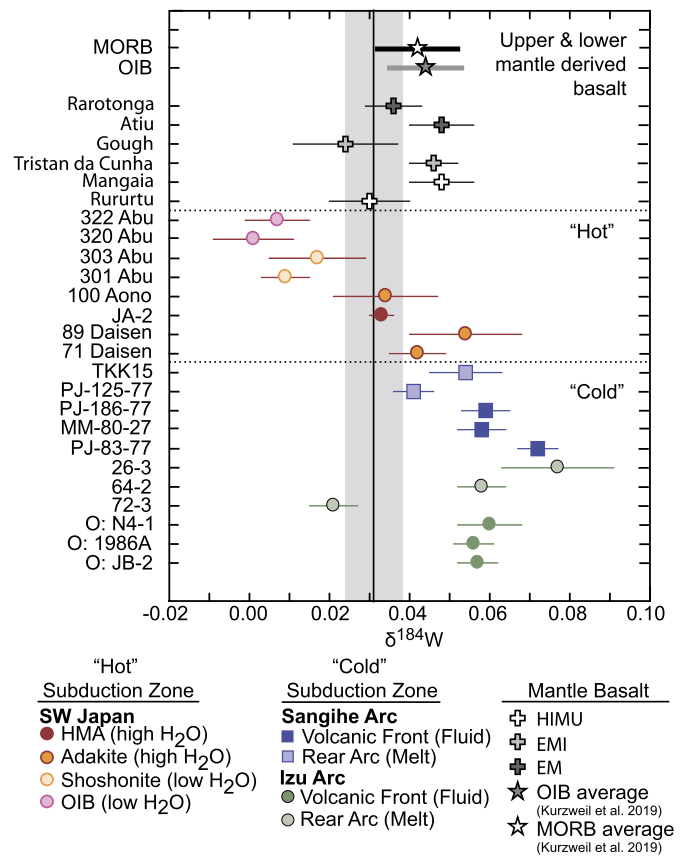


Fig. 4. $\delta^{184}\text{W}$ results for arc lavas analyzed in this study. O: Oshima. Error bars denote 95% confidence. Gray line and shaded region indicates chondritic $\delta^{184}\text{W}$ with 95% confidence to represent BSE (Krabbe et al., 2017). MORB and OIB data from Kurzweil et al. (2019).

Greber et al., 2015). It is likely that the same holds true for W, given the similar geochemical behavior and coordination of W and Mo in silicate melts, and the higher atomic mass of W compared to Mo. Core formation, therefore, likely did not influence the W stable isotope composition of the BSE, which should then be the same as the average chondritic $\delta^{184}\text{W}$ value of $0.031 \pm 0.007\%$ (Krabbe et al., 2017).

Moreover, if partial melting does not result in significant W isotope fractionation, the W stable isotope composition of the mantle should be identical to that of the BSE. Tungsten and Th are similarly incompatible during mantle melting (Arevalo and McDonough, 2008), and in the absence of experimentally determined partition coefficients for W in mafic melts, we use the bulk D for Th in peridotite (0.003, e.g., Salters and Stracke, 2004) to investigate W isotope fractionation during mantle melting. At 2% partial melting, 99.9% of the W is in the melt, and thus the $\delta^{184}\text{W}$ in the partial melt is identical to the melted mantle source (Supplementary Table 2). The generation of MORB requires 5–10% melting of a peridotite source (e.g., Salters and Stracke, 2004), and therefore partial melting of Earth's mantle does not result in any W stable isotope fractionation, independent of the assumed isotope fractionation factor, because all of the W is transferred quantitatively into the melt. The $\delta^{184}\text{W}$ of the Earth's mantle should, therefore, be the same as the value of BSE, which in turn should be chondritic.

Consistent with this expectation, the average $\delta^{184}\text{W}$ values of MORB and OIBs show no systematic departure from the chondritic $\delta^{184}\text{W}$ value (Fig. 4). Kurzweil et al. (2019) reported $\delta^{184}\text{W}$ for OIB from the Canary Islands and Réunion Island that cover a narrow range, with an average of $\delta^{184}\text{W}$ $0.042 \pm 0.009\%$, analytically indistinguishable from the chondritic $\delta^{184}\text{W}$ (Krabbe et al., 2017).

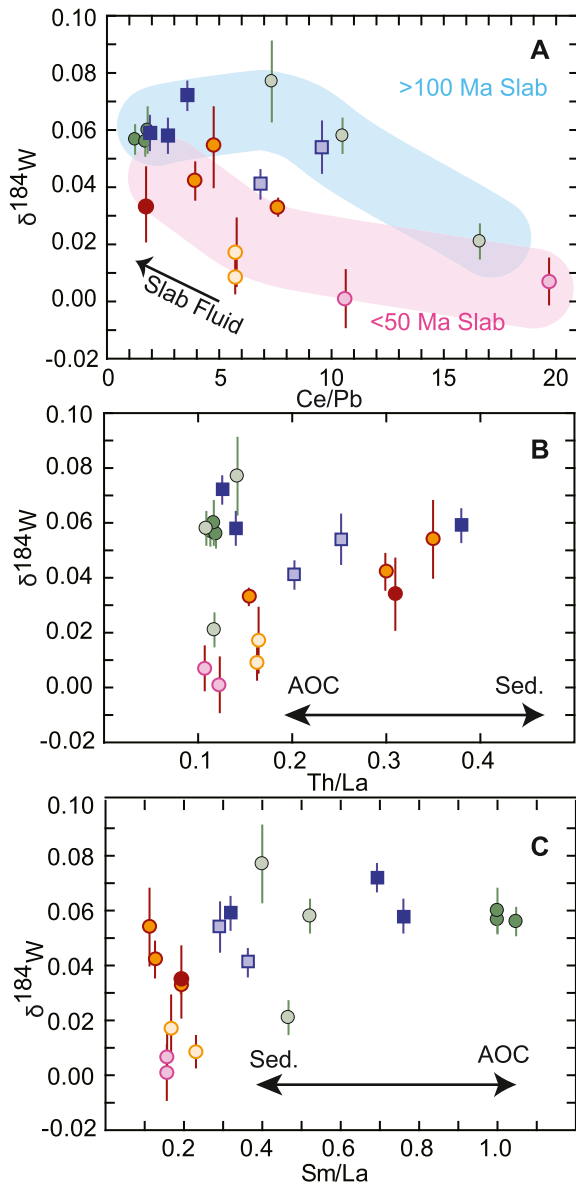


Fig. 5. A) $\delta^{184}\text{W}$ versus Th/La to indicate sediment component. B) $\delta^{184}\text{W}$ versus Sm/La to indicate AOC component. C) $\delta^{184}\text{W}$ versus Ce/Pb to indicate amount of aqueous fluid fluxing agent from subducting slab. Legend in Fig. 4.

Kurzweil et al. (2019) also report a narrow range in $\delta^{184}\text{W}$ values for mid-ocean ridge basalts (MORB), with an average of $\delta^{184}\text{W}$ $0.044 \pm 0.009\%$. Nevertheless, the OIBs from the present study display small $\delta^{184}\text{W}$ variations, including samples with slightly heavier W isotope compositions compared to BSE and the bulk mantle (Fig. 4). The $\delta^{184}\text{W}$ of OIBs that fall in different radiogenic isotope categories do not show systematic differences between different mantle reservoirs. This observation suggests that these small variations likely result from the recycling of crustal material with variable $\delta^{184}\text{W}$ into the mantle (see discussion below).

5.2. Origin of W isotope fractionation in arc lavas

Samples from ‘cold’ subduction zones (Izu and Sangihe arcs) are characterized by the heaviest $\delta^{184}\text{W}$ values, while ‘hot’ subduction zones (SW Japan) have progressively lighter $\delta^{184}\text{W}$ values (Fig. 4). The thermal conditions determine whether the slab-derived liquids are fluids or melts. The flux during shallow magma genesis is a dilute aqueous fluid that becomes more melt-like with depth (e.g., Plank et al., 2009). Enrichment of more fluid-mobile elements

(e.g., Pb, Ba, U, Cs) versus melt-mobile elements (e.g., REE, Th) potentially identifies the nature of the slab fluxing agent, and thermal conditions, in arc volcanics (Fig. 2). The volcanic fronts of the investigated ‘cold’ subduction zones are fluid-rich and the rear arcs are melt-rich (Hanyu et al., 2012; Tollstrup et al., 2010). If the nature of the slab fluxing agent is responsible for the observed $\delta^{184}\text{W}$ signatures, we would expect a correlation between $\delta^{184}\text{W}$ and diagnostic trace element ratios indicative of increasing temperatures in the subducting slab.

The volcanic front lavas of the ‘cold’ arcs analyzed here have higher Ba/La, Ba/Th, and $\delta^{184}\text{W}$ values than their rear arc lavas, and lower Ce/Pb (Fig. 5, Fig. 6). However, in the ‘hot’ subduction zones analyzed here there is no correlation between Ba/La and Ba/Th with $\delta^{184}\text{W}$ values, although there is a correlation between increased Ce/Pb and lighter $\delta^{184}\text{W}$ values. The Ba/La or Ba/Th of the produced arc lavas also depend on the variable stability of accessory minerals like phengite (Hanyu et al., 2012; Tollstrup et al., 2010), and may thus not be unambiguous indicators of fluid versus melt.

The $\delta^{184}\text{W}$ signature in arc magmas may also be influenced by the kind and relative amount of sediment in the source of the slab liquid, or the mass fraction (F) of the slab liquid added to the mantle wedge. For the ‘cold’ arcs, the volcanic front is characterized by AOC-like trace element signatures (high Sm/La), while the rear arc lavas are more enriched in sediment-derived trace elements (high Th/La) (Supplementary Fig. 3). Southwest Japan is especially enriched in Th/La indicating a pronounced sediment signature in the slab source (Supplementary Fig. 3). The lack of correlation between Th/La and $\delta^{184}\text{W}$ values thus suggests that the proportion of sediment component in the slab liquid does not control the $\delta^{184}\text{W}$ signature in the SW Japan arc (Fig. 5b). The heaviest $\delta^{184}\text{W}$ values from SW Japan (in Daisen adakites) is associated with 80% sediment in the slab source (Kimura et al., 2014), which is within analytical error of the $\delta^{184}\text{W}$ values of the Izu and Sangihe samples where the calculated percent sediment in the slab source is similar or much smaller ($\sim 20\%$ for Sangihe, Hanyu et al., 2012; $\sim 5\%$ for Izu; Tollstrup et al., 2010) (Fig. 3b). Similar to the lack of correlation of $\delta^{184}\text{W}$ with the proportion of sediment in the slab liquid (Fig. 3b), there is also no systematic relation between the $\delta^{184}\text{W}$ values and the inferred mass fraction of slab liquid (Fig. 3c), suggesting that neither the amount of sediment nor the mass fraction of slab liquid controls $\delta^{184}\text{W}$ signatures in arcs.

Observed variations in W/Th reflect the fluid mobile nature of W in subduction zones (König et al., 2008). Elevated W/Th, i.e., greater than those estimated for the MORB mantle (~ 0.18 , Kurzweil et al., 2019), may thus indicate W enrichment by fluids in the arc source. However, the arc lavas presented here show no correlation between $\delta^{184}\text{W}$ values and W/Th ratios. The full range of $\delta^{184}\text{W}$ values is observed in arc samples with W/Th similar to MORB and OIB (Fig. 7). Only lavas from Izu are characterized by the high W/Th ratios, and while most of these elevated W/Th ratios are coupled with heavy $\delta^{184}\text{W}$ values, the lightest $\delta^{184}\text{W}$ values are observed in a sample (72-3) that is melt dominated (Tollstrup et al., 2010), making it difficult to use W/Th ratios as an indicator of fluids.

Sediments could also control the $\delta^{184}\text{W}$ signatures recorded in arc lavas, due to the affinity for ferro-manganese oxides (FMOs) to absorb light W isotopes during FMO precipitation (Kashiwabara et al., 2017). If FMOs are the source of the $\delta^{184}\text{W}$ signature in arc volcanics, we would expect that light $\delta^{184}\text{W}$ values are associated with increasing sediment component, which is not the case (Fig. 3b, Fig. 5b). Alternatively, the inferred heavy $\delta^{184}\text{W}$ signature of modern seawater resulting from the precipitation of light W isotopes onto FMOs, (Kashiwabara et al., 2017) suggests that the seawater-altered parts of the slab (AOC and serpentinites) also have heavy $\delta^{184}\text{W}$ values. If so, our data suggest that AOC does

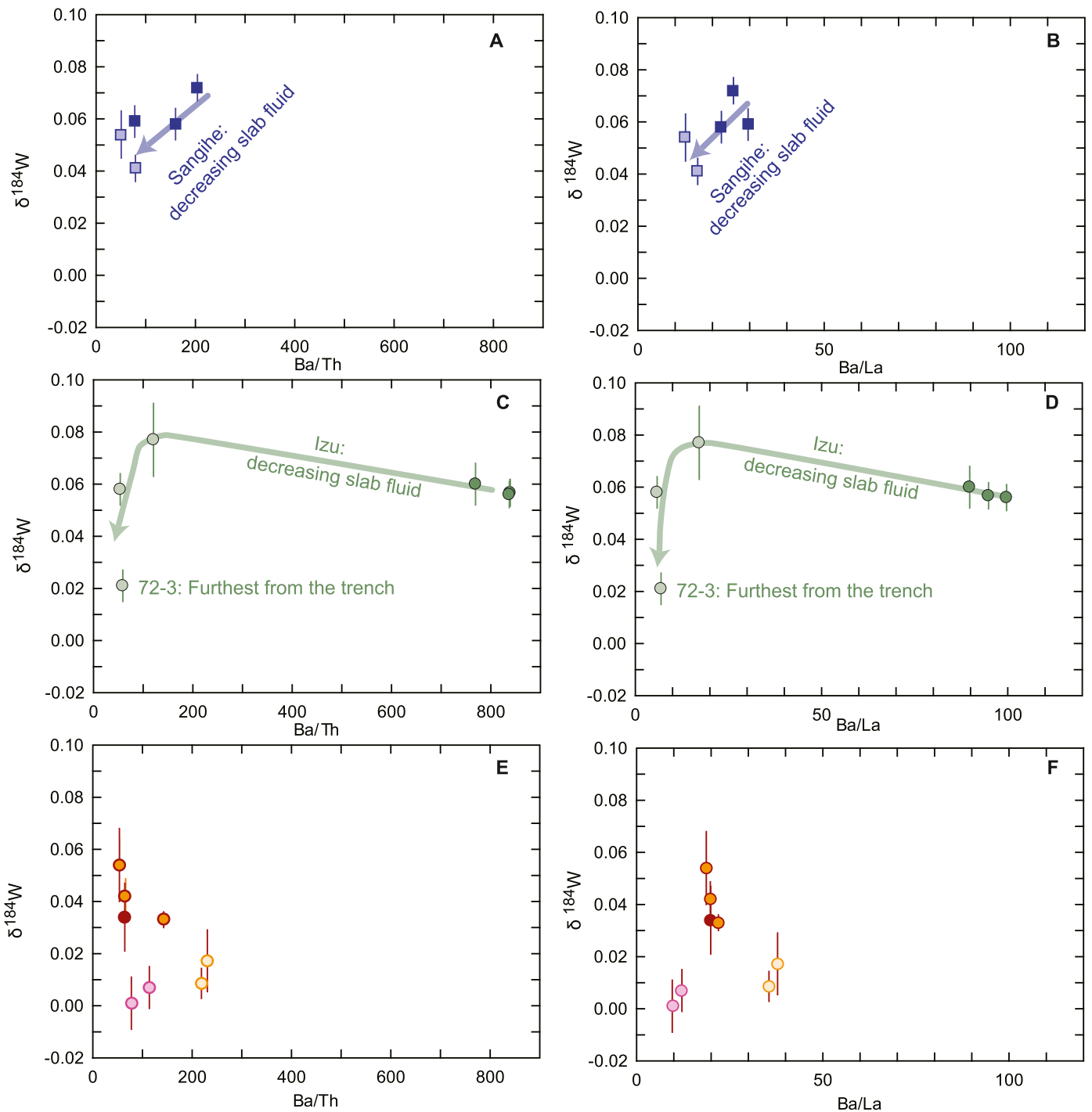


Fig. 6. **A & B)** Ba/Th and Ba/La versus $\delta^{184}\text{W}$ showing decreased slab-fluid component associated with lighter $\delta^{184}\text{W}$ values for the Sangihe arc. **C & D)** Ba/Th and Ba/La versus $\delta^{184}\text{W}$ showing decreased slab-fluid component associated with lighter $\delta^{184}\text{W}$ values for the Izu arc. **E & F)** Ba/Th and Ba/La versus $\delta^{184}\text{W}$ showing no correlation between slab-fluids and $\delta^{184}\text{W}$ composition for SW Japan. Legend in Fig. 4.

not control the $\delta^{184}\text{W}$ signature in arc lavas, because samples with the strongest AOC signature (Izu volcanic front) have $\delta^{184}\text{W}$ values indistinguishable from samples with the weakest AOC signature (adakites from SW Japan) (Fig. 5c). However, the dehydration of serpentinite in the subducted mantle lithosphere could also be carrying the inferred heavy $\delta^{184}\text{W}$ signature of seawater, therefore the extent of serpentinite controlling the $\delta^{184}\text{W}$ isotope composition of arc lavas needs to be further explored.

Rutile (TiO_2) is an important accessory phase in the slab, and because W substitutes for Ti (Zack et al., 2002), residual rutile may also fractionate W isotopes during subduction. The predominate

oxidation state of W in granitic melts is 6^+ , independent of oxygen fugacity (Che et al., 2013). If the substitution of W for Ti^{4+} in rutile results in a change of the W oxidation state from 6^+ to 4^+ , W in rutile should be isotopically light, because heavy isotopes prefer stronger bonding environments such as higher oxidation states (e.g., Schauble, 2004). Thus, if rutile is a residual phase during slab melting (e.g. Sangihe and Izu arcs), it would preferentially retain isotopically light $\delta^{184}\text{W}$, resulting in an isotopically heavy composition for the melt. Conversely, when slab temperatures are high enough to melt rutile, the melts should inherit isotopically light W from rutile. However, there is no simple correlation between

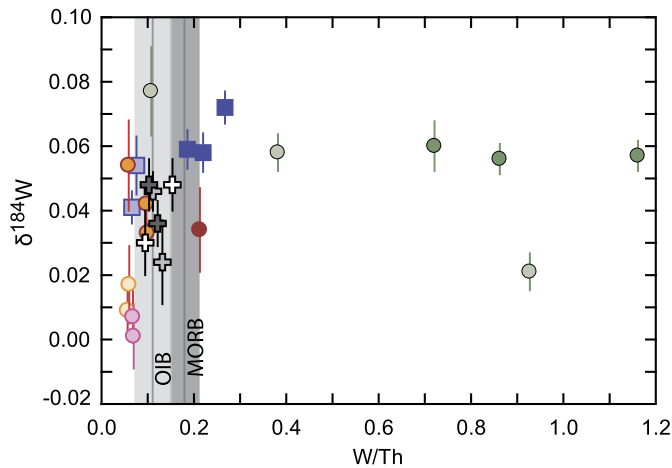


Fig. 7. $\delta^{184}\text{W}$ versus W/Th ratios for all samples analyzed. There is no correlation between $\delta^{184}\text{W}$ values and W/Th ratios. Grey bars correspond to OIB and MORB average W/Th (2 s.d.) from Kurzweil et al., 2019. Legend in Fig. 4.

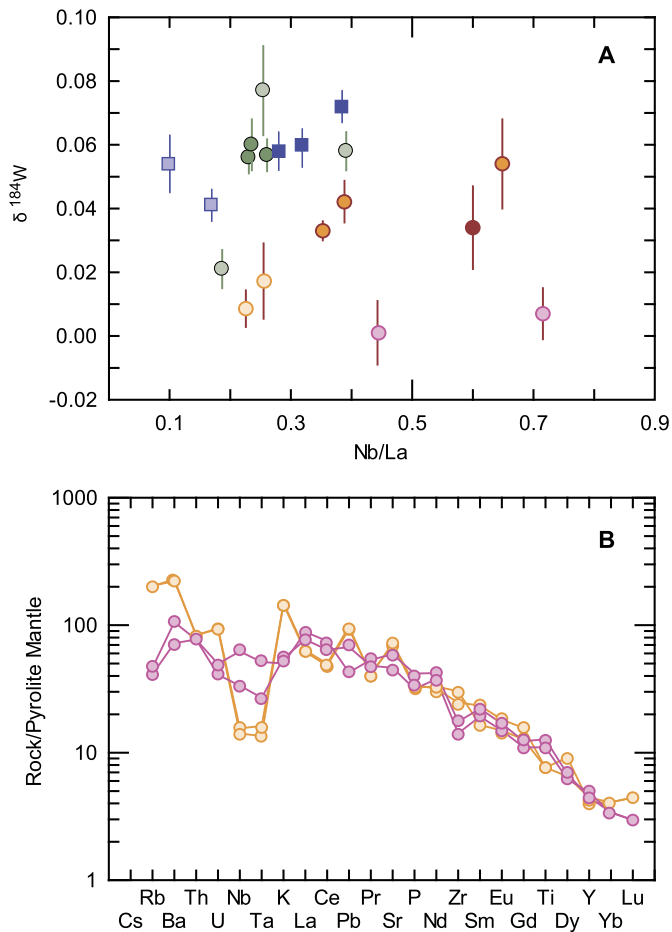


Fig. 8. **A)** Nb/La versus $\delta^{184}\text{W}$ for SW Japan, Sangihe, and Izu arcs. **B)** Pyrolite mantle normalized spider diagram for the dry lithologies from SW Japan. Legend in Fig. 4.

the extent of $\delta^{184}\text{W}$ fractionation and the magnitude of the Nb-depletion relative to similarly incompatible elements (e.g., Nb/La), which is a measure of the amount of residual rutile (Fig. 8). Although the OIB-like basalts have high Nb/La (0.71) and the lightest $\delta^{184}\text{W}$ values, the shoshonites have similar $\delta^{184}\text{W}$ values yet low Nb/La (<0.25) (Fig. 8). Therefore, on the basis of the data presented here, the role of rutile for $\delta^{184}\text{W}$ fractionation in subduction zones remains ambiguous.

The above discussion for both FMOs and rutile highlights the importance of understanding W carrier phases and how those phases could affect $\delta^{184}\text{W}$ fractionation in magmatic settings. Liu et al. (2018) conducted a reconnaissance study of W reservoirs in silicate rocks and found that pristine ultramafic rocks host W in olivine and orthopyroxene, while metasomatized mantle rocks host W in rutile and along grain boundaries. Tungsten mobility in fluids may result in increased W concentrations in metasomatic rocks, including metasomatism in the sub-arc mantle. While this study did not analyze any metasomatized samples, future studies should investigate the effects of metasomatism and W isotope fractionation in the sub-arc mantle. Other phases could be carriers of W, such as Os-Ir alloys (Babechuk et al., 2010), but due to the oxidized nature of the sub-arc mantle (Kelley and Cottrell, 2009) Os-Ir alloys are unlikely to affect W mobility and $\delta^{184}\text{W}$ fractionation because there would be no alloys present that could incorporate W and thus store the W in the slab. Furthermore, the oxidation state of subduction zones may affect the isotope fractionation of redox sensitive elements, but Kurzweil et al. (2019) showed that differences in $f\text{O}_2$ during partial melting do not produce resolvable differences in W stable isotope compositions.

In summary, there is no obvious correlation between $\delta^{184}\text{W}$ values and indicators of sediment melting in the arc lavas investigated in this study, suggesting that sediment and thus the light $\delta^{184}\text{W}$ values predicted for FMOs do not control the $\delta^{184}\text{W}$ fractionation in subduction zones. Other possible carrier phases of W such as Os-Ir alloys are also unlikely to affect $\delta^{184}\text{W}$ fractionation in subduction zones, while the role of rutile remains inconclusive at this stage for its potential to affect the W isotope composition in arc lavas. Instead, the arc lavas investigated here suggest that $\delta^{184}\text{W}$ values are correlated with the release of hydrous fluids from the subducting slab, suggesting that slab dehydration is the dominant process resulting in the observed W isotope fractionations.

5.3. Tungsten isotope ratios as tracers of progressive slab dehydration

Owing to the breakdown of phengite and the associated release of Ba, Ce/Pb is a better tracer for fluid/melt mobility than Ba/La in both 'cold' and 'hot' subduction zones. An increase in Ce/Pb, therefore, corresponds to an increase in the melt and a decrease in the mass fraction of slab-derived liquid (Chauvel et al., 1995). For the investigated 'cold' arcs (Sangihe and Izu), the heaviest $\delta^{184}\text{W}$ values occur in the volcanic front and up to 70 km behind it, in rocks with strong slab-fluid \pm moderate slab-melt characteristics. The across-arc geochemical variations have been attributed to a combination of more fluid from a less dehydrated slab beneath the volcanic front, and a higher temperature of melting of an increasingly dehydrated slab with increasing distance behind the front (Hochstaedter et al., 2001). Hence, $\delta^{184}\text{W}$ values likely trace slab dehydration, with heavy $\delta^{184}\text{W}$ compositions linked to high amounts of slab fluid leaving the increasingly dry residual slab with lighter $\delta^{184}\text{W}$ values, which can be recycled into the mantle.

For the investigated 'hot' subduction zone (SW Japan), $\delta^{184}\text{W}$ values becomes increasingly light in the sequence Daisen adakite > HMA (JA-2) > Aono adakite > shoshonite > OIB-like basalt. We interpret this sequence to reflect a decreasing amount of slab components (including slab H_2O) and melt derived from an increasingly drier source, in agreement with the conclusions of a previous study (Fig. 3; Kimura et al., 2014). The shoshonite and OIB-like basalt have the least slab component and represent the driest melts (Kimura et al., 2014), which results in the lightest $\delta^{184}\text{W}$ values reported in this study. In the case of SW Japan, our data suggests that heavy W isotopes are preferentially removed from the slab during dehydration, leaving the residual slab en-

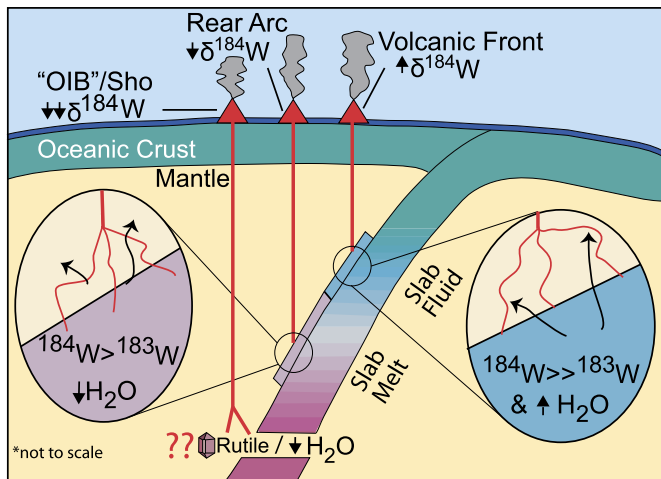


Fig. 9. Schematic diagram of a subduction zone displaying $\delta^{184}\text{W}$ fractionation corresponding to dehydration in arc magmatism. Aqueous fluids released during dehydration of the subducting slab fractionate heavy $\delta^{184}\text{W}$, while the remaining slab retains light $\delta^{184}\text{W}$ (potentially recorded in rutile). Drier melting and/or the melting of rutile associated with hot subduction and/or slab tear records the residual light $\delta^{184}\text{W}$. Black arrows correspond to relative mass movement, i.e. $\uparrow\text{H}_2\text{O}$ indicates high amounts of water being transferred out of the slab.

riched in light W isotopes, which are subsequently released during dry melting of the slab.

Finally, the W isotope composition of the down going slab could be variable, that is, depending on the extent of dehydration it may have heavy or light $\delta^{184}\text{W}$. Subduction of oceanic lithosphere with variable $\delta^{184}\text{W}$, in addition to continental crust with variable, arc-related variation in $\delta^{184}\text{W}$ also provides a potential way to produce the small W stable isotope heterogeneities in the mantle sources of some OIBs observed in this study (Fig. 4).

6. Conclusions

In all three investigated arcs, $\delta^{184}\text{W}$ is independent of slab composition (sediment vs. AOC) but is instead related to the amount of aqueous fluid and the thermal conditions of the subducting slab: low temperature, shallow, aqueous-fluid-rich lavas have heavy $\delta^{184}\text{W}$ signatures, leaving the dehydrated slab with residual light $\delta^{184}\text{W}$ signature, which is observed in lavas associated with increasing temperature, deeper melting, and lower slab-water content (Fig. 9).

The numerical models of van Keken et al. (2011) predict that most H_2O is released from the subducting slab between 100 km and 230 km depth, resulting in fluxing of the mantle wedge beneath the volcanic front and adjacent rear arc. Their models predict that H_2O is recycled into the mantle to >230 km depth in Izu, whereas the slab in SW Japan is completely dry by 150 km depth (van Keken et al., 2011: Fig. 7). The W isotope data of this study empirically supports these models, suggesting that W with heavy $\delta^{184}\text{W}$ signatures is removed from the slab during the initial dehydration under the volcanic front, and that a progressive increase to lighter $\delta^{184}\text{W}$ reflects further dehydration and increasing melting of the residual slab containing light $\delta^{184}\text{W}$ (Kimura et al., 2014, 2015), which is ultimately recycled into the deeper mantle.

Variables such as the W isotope composition of seawater, altered mantle lithosphere (i.e. subducted serpentinites), and rutile likely play an important role in the W isotope fractionation observed in arc magmas. To fully disentangle the processes related to W isotope fractionation from dehydration or inherited W isotope compositions released from the subducting slab, the W isotope composition and W concentration in subducting lithologies are needed. Nonetheless, our data suggests that heavy $\delta^{184}\text{W}$ prefer-

entially fractionates into fluid-rich magmas in modern subduction zones, suggesting that $\delta^{184}\text{W}$ signatures in arc lavas could trace the onset of cold subduction, and hence modern-style plate tectonics.

Declaration of competing interest

The authors declare that they have no known competing financial interests or personal relationships that could have appeared to influence the work reported in this paper.

Acknowledgements

We thank Heye Freymuth and Takeshi Hanyu for providing samples. We also thank Rajdeep Dasgupta for editorial handling and two anonymous reviewers whose comments helped improve this manuscript. This research received funding to T.K. from the E.R.C. under the European Community's Seventh Framework Programme (FP7/2007–2013 Grant Agreement 616564 'ISOCORE').

Appendix A. Supplementary material

Supplementary material related to this article can be found online at <https://doi.org/10.1016/j.epsl.2019.115942>.

References

- Abraham, K., Barling, J., Siebert, C., Belshaw, N., Gall, L., Halliday, A.N., 2015. Determination of mass-dependent variations in tungsten stable isotope compositions of geological reference materials by double-spike and MC-ICPMS. *J. Anal. At. Spectrom.* 30 (11), 2334–2342.
- Ando, A., Mita, N., Terashima, S., 1987. 1986 values for fifteen GSJ rock reference samples: Igneous Rock Series. *Geostand. Newsl.* 11 (2), 159–166.
- Arevalo, R., McDonough, W.F., 2008. Tungsten geochemistry and implications for understanding the Earth's interior. *Earth Planet. Sci. Lett.* 272 (3), 656–665.
- Babechuk, M.G., Kamber, B.S., Greig, A., Canil, D., Kodolanyi, J., 2010. The behavior of tungsten during mantle melting revisited with implications for planetary differentiation time scales. *Geochim. Cosmochim. Acta* 74 (4), 1448–1470.
- Bali, E., Keppler, H., Audetat, A., 2012. The mobility of W and Mo in subduction zone fluids and the Mo–W–Th–U systematics of island arc magmas. *Earth Planet. Sci. Lett.* 351, 195–207.
- Breton, T., Quitté, G., 2014. High-precision measurements of tungsten stable isotopes and application to Earth sciences. *J. Anal. At. Spectrom.* 29 (12), 2284–2293.
- Burkhardt, C.N., Hin, R.C., Kleine, T., Bourdon, B., 2014. Evidence for Mo isotope fractionation in the solar nebula and during planetary differentiation. *Earth Planet. Sci. Lett.*, 201–211.
- Chauvel, C., Goldstein, S.L., Hofmann, A.W., 1995. Hydration and dehydration of oceanic crust controls Pb evolution in the mantle. *Chem. Geol.* 126 (1), 65–75.
- Che, X.D., Linnen, R.L., Wang, R.C., Aseri, A., Thibault, Y., 2013. Tungsten solubility in evolved granitic melts: an evaluation of magmatic wolframite. *Geochim. Cosmochim. Acta* 106, 84–98.
- French, S.W., Romanowicz, B., 2015. Broad plumes rooted at the base of the Earth's mantle beneath major hotspots. *Nature* 525 (7567), 95–99.
- Freymuth, H., Ivko, B., Gill, J.B., Tamura, Y., Elliott, T., 2016. Thorium isotope evidence for melting of the mafic oceanic crust beneath the Izu arc. *Geochim. Cosmochim. Acta* 186, 49–70.
- Gill, J.B., 1981. *Orogenic Andesites and Plate Tectonics*. Springer, Heidelberg, Germany, 385 p.
- Greber, N.D., Puchtel, I.S., Nägler, T.F., Mezger, K., 2015. Komatiites constrain molybdenum isotope composition of the Earth's mantle. *Earth Planet. Sci. Lett.* 421, 129–138.
- Grove, T.L., Till, C.B., Krawczynski, M.J., 2012. The role of H_2O in subduction zone magmatism. *Annu. Rev. Earth Planet. Sci.* 40, 413–439.
- Hanyu, T., Gill, J., Tatsumi, Y., Kimura, J.I., Sato, K., Chang, Q., Senda, R., Miyazaki, T., Hirahara, Y., Takahashi, T., Zulkarnain, I., 2012. Across- and along-arc geochemical variations of lava chemistry in the Sangihe arc: various fluid and melt slab fluxes in response to slab temperature. *Geochem. Geophys. Geosyst.* 13 (10).
- Hin, R.C., Burkhardt, C., Schmidt, M.W., Bourdon, B., Kleine, T., 2013. Experimental evidence for Mo isotope fractionation between metal and silicate liquids. *Earth Planet. Sci. Lett.* 379, 38–48.
- Hochstaedter, A., Gill, J.B., Peters, R., Broughton, P., Holden, P., Taylor, B., 2001. Across-arc geochemical trends in the Izu-Bonin arc: contributions from the subducting slab. *Geochem. Geophys. Geosyst.* 2.

- Irisawa, K., Hirata, T., 2006. Tungsten isotopic analysis on six geochemical reference materials using multiple collector-ICP-mass spectrometry coupled with a rhenium-external correction technique. *J. Anal. At. Spectrom.* 21 (12), 1387–1395.
- Jackson, M.G., Dasgupta, R., 2008. Compositions of HIMU, EM1, and EM2 from global trends between radiogenic isotopes and major elements in ocean island basalts. *Earth Planet. Sci. Lett.* 276 (1–2), 175–186.
- Kashiwabara, T., Kubo, S., Tanaka, M., Senda, R., Iizuka, T., Tanimizu, M., Takahashi, Y., 2017. Stable isotope fractionation of tungsten during adsorption on Fe and Mn (oxyhydr)oxides. *Geochim. Cosmochim. Acta* 204, 52–67.
- Kelley, K.A., Cottrell, E., 2009. Water and the oxidation state of subduction zone magmas. *Science* 325 (5940), 605–607.
- Kimura, J.I., Kent, A.J., Rowe, M.C., Katakuse, M., Nakano, F., Hacker, B.R., van Keken, P.E., Kawabata, H., Stern, R.J., 2010. Origin of cross-chain geochemical variation in quaternary lavas from the northern Izu arc: using a quantitative mass balance approach. to identify mantle lavas from the northern Izu arc: using a quantitative mass balance approach to identify mantle sources and mantle wedge processes. *Geochem. Geophys. Geosyst.* 11 (10).
- Kimura, J.I., Gill, J.B., Kunikiyo, T., Osaka, I., Shimoshioiri, Y., Katakuse, M., Kakubuchi, S., Nagao, T., Furuyama, K., Kamei, A., Kawabata, H., 2014. Diverse magmatic effects of subducting a hot slab in SW Japan: results from forward modeling. *Geochem. Geophys. Geosyst.* 15 (3), 691–739.
- Kimura, J.I., Miyazaki, T., Vaglarov, B.S., Haraguchi, S., Chang, Q., Gill, J.B., 2015. Reply to comment by I. Pineda-Velasco, T.T. Nguyen, H. Kitagawa, and E. Nakamura on “Diverse magmatic effects of subducting a hot slab in SW Japan: results from forward modeling”. *Geochem. Geophys. Geosyst.* 16.
- König, S., Münker, C., Schuth, S., Garbe-Schönberg, D., 2008. Mobility of tungsten in subduction zones. *Earth Planet. Sci. Lett.* 274 (1–2), 82–92.
- König, S., Münker, C., Hohl, S., Paulick, H., Barth, A.R., Lagos, M., Pfänder, J., Büchl, A., 2011. The Earth's tungsten budget during mantle melting and crust formation. *Geochim. Cosmochim. Acta* 75 (8), 2119–2136.
- Krabbe, N., Kruijer, T.S., Kleine, T., 2017. Tungsten stable isotope compositions of terrestrial samples and meteorites determined by double spike MC-ICPMS. *Chem. Geol.* 450, 135–144.
- Kurzweil, F., Münker, C., Tusch, J., Schoenberg, R., 2018. Accurate stable tungsten isotope measurements of natural samples using a 180W-183W double-spike. *Chem. Geol.* 476, 407–417.
- Kurzweil, F., Münker, C., Grupp, M., Braukmüller, N., Fechtner, L., Christian, M., Hohl, S.V., Schoenberg, R., 2019. The stable tungsten isotope composition of modern igneous reservoirs. *Geochim. Cosmochim. Acta* 251, 176–191.
- Liu, J., Pearson, D.G., Chacko, T., Luo, Y., 2018. A reconnaissance view of tungsten reservoirs in some crustal and mantle rocks; implications for interpreting W isotopic compositions and crust-mantle W cycling. *Geochim. Cosmochim. Acta* 223, 300–318.
- Morrice, M.G., Jezek, P.A., Gill, J.B., Whitford, D.J., Monoarfa, M., 1983. An introduction to the Sangihe arc: volcanism accompanying arc-arc collision in the Molucca Sea, Indonesia. *J. Volcanol. Geotherm. Res.* 19 (1–2), 311–353.
- Newson, H.E., Sims, K.W., Noll Jr, P.D., Jaeger, W.L., Maehr, S.A., Beserra, T.B., 1996. The depletion of tungsten in the bulk silicate earth: constraints on core formation. *Geochim. Cosmochim. Acta* 60 (7), 1155–1169.
- Plank, T., Cooper, L.B., Manning, C.E., 2009. Emerging geothermometers for estimating slab surface temperatures. *Nat. Geosci.* 2, 611–615.
- Rudge, J.F., Reynolds, B.C., Bourdon, B., 2009. The double spike toolbox. *Chem. Geol.* 265 (3–4), 420–431.
- Rudnick, R.L., Gao, S., 2003. Composition of the continental crust. In: *Treatise on Geochemistry*, vol. 3, pp. 1–64.
- Salters, V.J.M., Stracke, A., 2004. Composition of the depleted mantle. *Geochem. Geophys. Geosyst.* 5 (5).
- Schauble, E.A., 2004. Applying stable isotope fractionation theory to new systems. In: Johnson, C.M., Beard, B.L., Albarède, F. (Eds.), *Geochemistry of Non-Traditional Stable Isotopes*, vol. 55, pp. 65–111.
- Spandler, C., Pirard, C., 2013. Element recycling from subducting slabs to arc crust: a review. *Lithos* 170, 208–223.
- Stracke, A., 2012. Earth's heterogeneous mantle: a product of convection-driven interaction between crust and mantle. *Chem. Geol.* 330, 274–299.
- Syracuse, E.M., van Keken, P.E., Abers, G.A., 2010. The global range of subduction zone thermal models. *Phys. Earth Planet. Inter.* 183 (1–2), 73–90.
- Tatsumi, Y., Eggins, S., 1995. *Subduction Zone Magmatism*, vol. 1. Wiley.
- Tollstrup, D., Gill, J., Kent, A., Prinkey, D., Williams, R., Tamura, Y., Ishizuka, O., 2010. Across-arc geochemical trends in the Izu-Bonin arc: contributions from the subducting slab, revisited. *Geochem. Geophys. Geosyst.* 11 (1).
- van Keken, P.E., Hacker, B.R., Syracuse, E.M., Abers, G.A., 2011. Subduction factory: 4. Depth-dependent flux of H₂O from subducting slabs worldwide. *J. Geophys. Res., Solid Earth* 116 (B1).
- Willbold, M., Elliott, T., 2017. Molybdenum isotope variations in magmatic rocks. *Chem. Geol.* 449, 253–268.
- Willbold, M., Stracke, A., 2006. Trace element composition of mantle end-members: implications for recycling of oceanic and upper and lower continental crust. *Geochem. Geophys. Geosyst.* 7 (4).
- Wille, M., Nebel, O., Pettke, T., Vroon, P.Z., König, S., Schoenberg, R., 2018. Molybdenum isotope variations in calc-alkaline lavas from the Banda arc, Indonesia: assessing the effect of crystal fractionation in creating isotopically heavy continental crust. *Chem. Geol.* 485, 1–13.
- Zack, T., Kronz, A., Foley, S.F., Rivers, T., 2002. Trace element abundances in rutiles from eclogites and associated garnet mica schists. *Chem. Geol.* 184 (1–2), 97–122.
- Zhao, D., Yanada, T., Hasegawa, A., Umino, N., Wei, W., 2012. Imagining the subducting slabs and mantle upwelling under the Japan Islands. *Geophys. J. Int.* 190 (2), 816–828.
- Zindler, A., Hart, S., 1986. Chemical geodynamics. *Ann. Rev. Earth Planet. Sci.* 14 (1), 493–571.